

Efficient Simulation of Knitted Cloth Using Persistent Contacts

Gabriel Cirio

Jorge Lopez-Moreno

Miguel A. Otaduy

URJC Madrid



Figure 1: Yarn-level simulation of a knitted sweater with 56K loops (220K contact nodes, 1.1M DoFs), computed at 1.5 minutes per frame. Our model captures robustly and efficiently both the fine- and large-scale mechanics of knitted cloth.

Abstract

Knitted cloth is made of yarns that are stitched in regular patterns, and its macroscopic behavior is dictated by the contact interactions between such yarns. We propose an efficient representation of knitted cloth at the yarn level that treats yarn-yarn contacts as persistent, thereby avoiding expensive contact handling altogether. We introduce a compact representation of yarn geometry and kinematics, capturing the essential deformation modes of yarn loops and stitches with a minimum cost. Based on this representation, we design force models that reproduce the characteristic macroscopic behavior of knitted fabrics. We demonstrate the efficiency of our method on simulations with millions of degrees of freedom (hundreds of thousands of yarn loops), almost one order of magnitude faster than previous techniques.

CR Categories: I.3.5 [Computer Graphics]: Computational Geometry and Object Modeling—Physically based modeling

Keywords: Knitted cloth, Yarns, Physically based simulation

1 Introduction

The vast majority of garments are made of a yarn structure, either knitted or woven, and the macroscopic behavior of cloth is dictated by the mechanical interactions taking place at the yarn level. However, most cloth simulation models in computer graphics ignore the relevance of such yarn structure, represent the cloth surface as an arbitrary mesh, and compute internal elastic forces either by discretizing continuum elasticity models [Etmuss et al. 2003] or using discrete elastic elements [Breen et al. 1994; Provot 1995].

The seminal work of Kaldor et al. [2008] proposed an alternative approach for knitted cloth, describing individual yarns using a rod

model, and resolving contact interactions between yarns. A yarn-based model enables the simulation of complex small-scale effects, such as yarn-yarn friction and sliding, snags, pulls, frayed edges, or detailed fracture. Yet Kaldor et al. also showed that, with a yarn-based model, the macroscopic nonlinear mechanics of garments arise naturally through aggregation of yarn-level structural effects. But their method is hindered by a major challenge: efficient and robust detection and resolution of all yarn contacts. They later improved the performance of their approach by reusing linearized contact information whenever possible [Kaldor et al. 2010].

In this paper, we propose a representation of knitted cloth using persistent contacts with yarn sliding. With this representation, we achieve robust and efficient simulations, as we avoid the detection and resolution of yarn-yarn contacts altogether. On garments of similar complexity to those simulated by Kaldor et al. [2010], such as the sweater shown in Fig. 1, with over 56K stitch loops, we achieve a 7x speed-up (without accounting for hardware differences). But with our method we are also able to simulate much denser fabrics, up to common real-world gauges, such as the shirt in Fig. 8, with 325K loops.

Recently, Cirio et al. [2014] also proposed a yarn-level model for woven cloth based on persistent contacts. Indeed, our mathematical formulation of the dynamics equations builds strongly on the formulation of Cirio et al., but there are important differences too. There are fundamental structural differences in the arrangement of yarns in woven and knitted cloth, which produce different inter-yarn contact mechanics as well as different yarn-level deformation modes. Then, the persistent contact representation and force models of woven cloth are not directly applicable to knitted cloth. For Cirio et al., the placement of such persistent contacts and hence the discretization of the fabric could be naturally inferred from the woven structure. In our case, designing an effective discretization of knitted yarns using persistent contacts while retaining all the important degrees of freedom of the knitted structure was not straightforward. Defining yarn-level force models that capture the macroscopic behavior of knitted cloth was not trivial either.

We introduce a compact yarn-level representation of knitted fabrics, based on the placement of four persistent contacts with yarn sliding on each stitch. Following this representation, we design force models for inter-yarn friction, yarn bending, and stitch wrapping. We

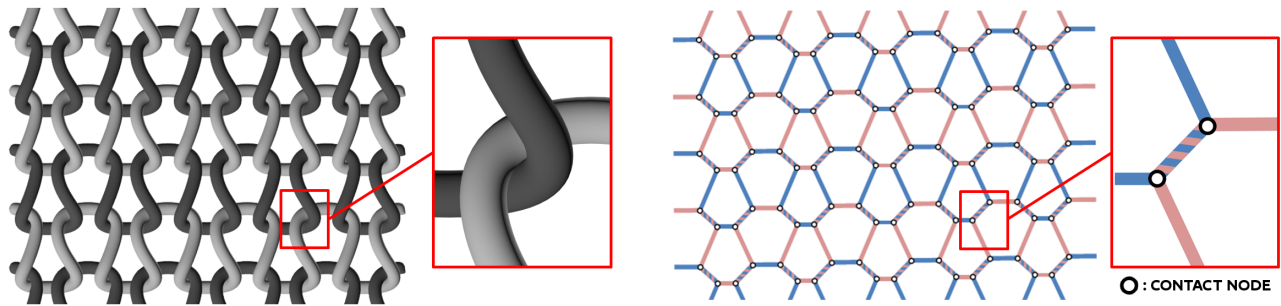


Figure 2: Images of a knit and its discretization. From left to right: loops of a knit in 3D, zoom on a stitch in 3D, discretization of the knit, and zoom on a discretized stitch with two persistent contacts.

have carried out experiments that evaluate the influence of yarn-level mechanical and geometric parameters on macroscopic mechanical behavior, and we observe the characteristic stretch, shear, and bending behavior of knitted fabrics, with manifest anisotropy, nonlinear stretch behavior, and plasticity.

2 Related Work

Yarn-level models of knitted and woven fabrics have a long history, dating back to 1937 when Peirce [1937] proposed a geometric model to represent the crossing of yarns in woven fabric. Yarn-level models have been thoroughly studied in the field of textile research, initially using analytical yarn models [Hearle et al. 1969] to predict the mechanical behavior of fabric under specific modes of deformation [Peirce 1937; Kawabata et al. 1973]. Later, textile research relied on continuum models to simulate most yarn deformation modes and complex yarn-yarn contact interactions [Ng et al. 1998; Page and Wang 2000; Duan et al. 2006]. A number of techniques have been developed to alleviate the large computational burden of yarn-level continuum models, such as using multiscale models that resort to costly yarn-level mechanics only when needed [Nadler et al. 2006], or replacing the complex volumetric yarns by simpler elements such as beams, trusses and membranes [Reese 2003; McGlockton et al. 2003].

Knitted fabric has received less attention compared to woven, perhaps due to the higher geometric complexity, which leads to more involved yarn contact interactions. Splines are often used to efficiently represent knit yarns, as introduced by Remion et al. [1999]. Splines have also been used to approximate woven fabric in a purely geometric way (see e.g., [Renkens and Kyosev 2011; Jiang and Chen 2005]), sometimes combined with thin sheet models in a multiscale fashion [Nocent et al. 2001].

Often, yarn-level models capture the most relevant deformations and yarn interactions using specialized force models, such as bending and crossover springs to capture cross-sectional deformation and shear at crossover points [King et al. 2005; Xia and Nadler 2011], truss elements acting as contact forces between yarns to capture shear jamming [King et al. 2005], or a slip velocity to capture yarn sliding [Parsons et al. 2013]. As a consequence, these models enable the simulation of realistic macroscopic behaviors of fabric. However, yarn-level models in textile research focus on small portions of fabric, often in controlled experiments, and cannot simulate entire garments under free motions, nor single yarn plastic effects such as snags, pulls and pullouts.

Recently, yarn-level models that address these shortcomings have emerged in the field of computer graphics. The seminal work of Kaldor et al. [2008] was the first approach capable of simulating entire garments at the yarn level in tractable time, from loose scarves

and leg warmers to large sweaters. Focusing on knits, they modeled the mechanics of individual yarns using inextensible rods, and computed yarn-yarn contact through stiff penalty forces and velocity-filter friction, allowing them to predict the large-scale behavior of full garments from fundamental yarn mechanics. They extended their work by using local rotated linearizations of penalty forces to accelerate yarn-yarn contact handling [Kaldor et al. 2010]. Yuksel et al. [2012], on the other hand, designed geometric methods to create simulation-ready yarn-level models of many knit patterns.

More recently, Cirio et al. [2014] focused on woven cloth by taking a different approach. They assume that yarn-yarn contacts are persistent in time, even under moderately large plastic deformations. This assumption avoids the need of expensive yarn-yarn collision detection and contact handling, thus greatly reducing simulation costs. They simulate every yarn in the fabric as a rod, and introduce additional sliding degrees of freedom at yarn crossings to allow yarns to slide along each other and thus generate complex plastic effects such as snags, pulls, fracture and frayed edges. Other yarn-level models (mainly geometric and analytical ones) also assumed persistent contact, but they did not incorporate sliding coordinates. Our work leverages the concept of persistent contact with sliding degrees of freedom and extends it to the other large family of fabrics, knitted cloth. Contacts in knitted fabric are more complex than in woven, hence it is not sufficient to represent each contact as one crossing node with sliding coordinates. Through observation of the deformation modes present in knit loops, we concluded that representing each stitch using four persistent contacts with yarn sliding would suffice to capture all the interesting deformation modes. This approach leads to a much more compact and efficient representation than previous work for knitted cloth, while still enabling all yarn-level interactions that produce interesting and realistic small- and large-scale behaviors.

Sueda et al. [2011] introduced a general formulation of Lagrangian mechanics to simulate efficiently the dynamics of highly constrained rods, through an optimal set of generalized coordinates that combine absolute motion with sliding on constraint manifolds. The model of persistent contacts designed by Cirio et al. [2014] constitutes an application of Sueda’s framework to the case of two rods in sliding contact.

3 Yarn Discretization

We propose a representation of knitted cloth using persistent contacts that is compact yet aims to capture the mechanically relevant characteristics of the yarn structure. We begin this section by summarizing this structure, with a focus on its influence on the macroscopic behavior of garments.

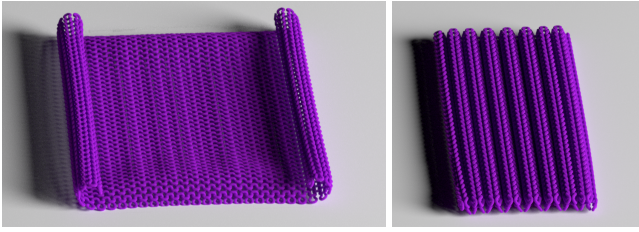


Figure 3: Curling behavior due to stitch unwrapping. Left: stockinette pattern. Right: rib pattern.

3.1 Structure of Knitted Fabrics

Kaldor et al. [2008] provide an excellent description of how yarns are stitched together to produce a knitted fabric and its behavior. We repeat only the most basic concepts before introducing our model.

A single yarn is laid out in a chain of loops along a row of the so-called *course* direction. These loops are pulled either up or down through the loops of the previous row, in a *knit* or *purl* stitch respectively. Loops appear stacked in columns on the *wale* direction. When the yarn reaches the end of a row, it is typically bent back to form the next row. The first and last row are stitched in a different way to avoid unraveling, while the beginning and end of a yarn are simply tied to the fabric. Fig. 2-left shows several loops of a fabric knitted in *stockinette* pattern, which is the simplest pattern, with all knit stitches. In the paper, we also show simulated examples of other patterns: *garter*, which alternates rows of knit and purl stitches, and *rib*, which repeats two knit stitches followed by two purl stitches. We refer the reader to the paper by Kaldor et al. [2008] for representative images of each knit pattern.

Yarns of a knitted fabric undergo multiple different forces, both internal due to their own deformation, and external due to yarn-yarn contact. The macroscopic mechanical behavior of knitted garments is largely determined by yarn-yarn contact, with three dominating effects: (i) contact at stitches, with yarns wrapped around each other, (ii) contact between adjacent loops when a stitch tightens, and (iii) friction under inter-yarn sliding or shear. Macroscopic in-plane deformation (i.e., stretch and shear) of a garment is dominated first by the bending resistance of yarns as loops deform, then adjacent loops may enter into contact, and finally additional deformation requires stretching the yarns themselves. When a knitted fabric is laid flat, elastic energy is present due to yarn bending and yarn wrapping. When the fabric is allowed to relax, it will undergo some macroscopic deformation. With a garter pattern, the bending deformation produced by stitch unwrapping is compensated on alternate rows and columns of loops. On a stockinette pattern, rows and columns curl in opposite directions (See Fig. 3-left). On a rib pattern, each pair of stitches curls in opposite direction, leading to a significant natural compression of the fabric (See Fig. 3-right).

In Section 4, we present force models that capture these essential yarn contact mechanics under our compact yarn representation, and we demonstrate how they reproduce the expected nonlinearity and anisotropy of knitted fabrics.

3.2 Discretization Using Contact Nodes

Our strategy to discretize yarns in a knitted fabric is to identify the minimum set of persistent contacts that allow representing all relevant deformation modes. Cirio et al. [2014] applied this strategy to woven fabrics, which they discretized by placing crossing nodes at the crossings of warp and weft yarns. At a crossing node, the two yarns in contact are represented as a single 3D point, thereby elim-

inating the need to detect and resolve contact. The crossing node is augmented with sliding coordinates that allow the yarns to slide tangent to the contact. We extend crossing nodes to other persistent contact configurations, and refer to them as *contact nodes*.

In a stitch, a loop from one row is passed through two loops of the previous row. This arrangement produces two stitch contacts, as shown in Fig. 2. During normal operation of the fabric, i.e., unless a stitch is pulled out, the two yarns at each stitch contact are wrapped around each other persistently. Based on this observation, we discretize knitted fabrics by placing two contact nodes at the two end points of each stitch contact, as shown in Fig. 2-right. This discretization captures the most important degrees of freedom in a loop, and allows us to represent any knit pattern based on purl and knit stitches between two yarns. Using a single contact node per stitch contact would miss important loop deformation modes, such as the stretching of fabric due to loop deformation.

For simulation purposes, we consider the yarn to be formed by straight segments between contact nodes. For rendering purposes, on each contact node we fit a plane to the incident segments, offset the yarns along the normal of this plane, and interpolate the resulting points using smooth splines.

Same as Cirio et al., we allow yarns to slide at persistent contacts, hence each contact node $\mathbf{q} = (\mathbf{x}, u, v)$ constitutes a 5-DoF node, with \mathbf{x} the 3D position of the node, and u and v the arc lengths of the two yarns in contact, which act as sliding coordinates. Each loop has typically 4 stitch contacts, hence it shares 8 contact nodes with other loops. As a result, a garment with N loops has approximately $4N$ contact nodes and $20N$ DoFs. We follow the framework of Sueda et al. [2011] to derive the equations of motion, linearly interpolating kinematic magnitudes along yarn segments and applying the Lagrange-Euler equations. We omit the full derivation here, which differs from Cirio’s only w.r.t. the force model.

4 Force Model

We now describe the forces applied on the knit model, which include gravity, internal elastic forces of yarns, non-penetration contact forces between yarns, friction, and damping. In our design of the specific force models, we have identified key deformation modes of the yarn structure that suffer resistance. In some cases, particularly for yarn bending, our force model groups the effect of both internal and contact forces. This is a crucial aspect in the design of force models with persistent contacts, because the lack of degrees of freedom in the normal direction of contacts prevents the use of typical penalty potentials or non-penetration constraints.

For gravity, yarn stretch (governed by the Elastic modulus Y), and contact between adjacent loops we use exactly the same formulations as Cirio et al. [2014]; therefore, we refer the reader to their paper for details. In our force model, we include elastic potentials for two major deformation modes, which we describe first: yarn bending and stitch wrapping. Next, we discuss details of sliding friction forces, although similar forces are added to all deformation modes. We conclude with the description of an elastic force for the preservation of the lengths of stitch contacts. For damping, we use the Rayleigh model.

According to textile literature [Duhovic and Bhattacharyya 2006], the contribution of dynamic yarn twisting is minor, especially compared to dominant forces such as stretch and bending. Therefore, following the general approach, we do not include yarn twist in our force model. Yarn pre-twisting, on the other hand, has an influence on other yarn parameters [Pan and Brookstein 2002]. We capture this effect by varying bending stiffness and yarn radius accordingly.

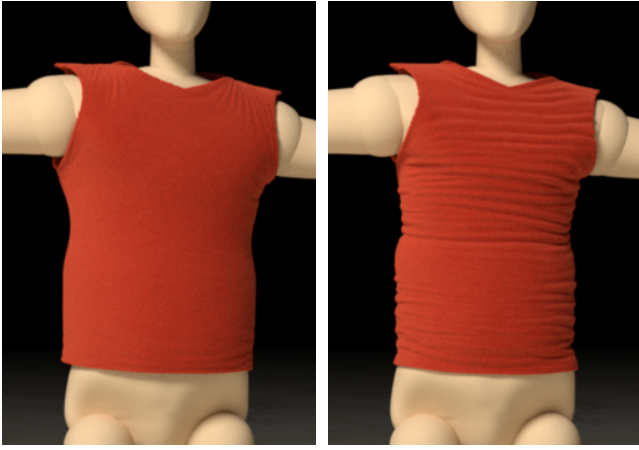


Figure 4: A knit shirt with (left) and without (right) rest-shape bending compensation. Without compensation, the garment shrinks and exhibits unnatural wrinkles.

The formulations of forces and their Jacobians, except for stitch wrapping, are equivalent to the ones derived by Cirio et al. for woven cloth. We provide full derivations of forces and Jacobians of stitch wrapping in the Appendix.

4.1 Yarn Bending

Given two consecutive yarn segments, we define an elastic potential based on the angle θ between them:

$$V = k_b \frac{\theta^2}{\Delta u}. \quad (1)$$

Here Δu is the summed arc length of both segments. For small angles, the bending stiffness is due to internal forces during yarn bending, and can be defined as $k_b = B\pi R^2$, with B the bending modulus and R the yarn radius. This is identical to the bending model implemented by Cirio et al. for woven cloth. Our bending model differs, however, for large bending angles. Under this situation, the deformation of loops leads to contact between loops of different rows, or *bending jamming*. We model this effect after the shear jamming of Cirio et al., by increasing the bending stiffness after a certain threshold ($\theta = \pi/2$ in our examples).

To initialize the yarn layout for a garment, we set the desired loop density in the course and wale directions, the yarn radius, and the geometric shape of a loop (i.e., the relative position of the nodes within a loop). The resulting layout may not be at rest in this initial configuration due to unbalanced bending energies, and the garment may compress and wrinkle when relaxed. We compensate for the rest-shape bending by redefining loop densities in the following way. We first relax a rectangular sample of 5×5 cm with the same mechanical and geometric parameters, and record the average shape of loops after relaxation. Then, we apply this loop shape in the initialization of the yarn layout for the garment, by redefining the loop density accordingly. Fig. 4 compares a piece of fabric with and without rest-shape bending compensation.

4.2 Stitch Wrapping

At each stitch contact, two yarn segments are wrapped around each other, as shown in Fig. 2, producing a deformation energy. Fig. 6 shows the wrapping in more detail, along with the notation we follow. We measure the amount of wrapping as the relative angle between opposite yarn segments around the central axis of the stitch



Figure 5: Knit garment with a stockinette pattern, with its characteristic curling behavior at the edges.

contact. Given the two contact nodes of the stitch contact, \mathbf{q}_0 and \mathbf{q}_1 , the unit vector \mathbf{e} between them defines the central axis. We define a wrapping angle ψ between the blue yarn segment from \mathbf{q}_0 to \mathbf{q}_4 and its opposite pink yarn segment from \mathbf{q}_1 to \mathbf{q}_3 , and similarly for the other two segments. Specifically, we compute the angle between the normals of the triangles (shown in light blue and light pink in the figure) formed by such yarn segments and the central axis, which acts as a hinge.

For each pair of opposite yarn segments, we define an elastic potential based on the deviation between the wrapping angle ψ and a rest angle ψ_0 :

$$V = \frac{1}{2} k_w L (\psi - \psi_0)^2, \quad (2)$$

where k_w is an empirically set stiffness, and L is the rest length of the stitch contact. After testing different values for ψ_0 , we chose $\pi/2$ for a visually realistic wrapping effect.

The yarn segments at stitch contacts have the natural tendency to unwrap. In the garter pattern, adjacent rows of loops unwrap in opposite directions. However, in the stockinette pattern, where they unwrap in the same direction, a characteristic behavior emerges: the fabric has a tendency to curl both in wale and course directions. This effect is particularly noticeable at the boundaries of the fabric, as shown in Fig. 3-left and Fig. 5. In the rib pattern, on the other hand, each pair of stitches curls in opposite direction, leading to a natural compression of the fabric, as shown in Fig. 3-right.

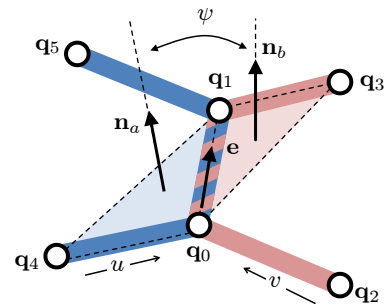


Figure 6: Representation of a stitch contact. \mathbf{q}_0 and \mathbf{q}_1 are the contact nodes of the stitch contact, with the blue and pink segments belonging to two different loops. We measure stitch wrapping as the angle ψ between the light blue and light pink triangles, with the central axis \mathbf{e} acting as a hinge.

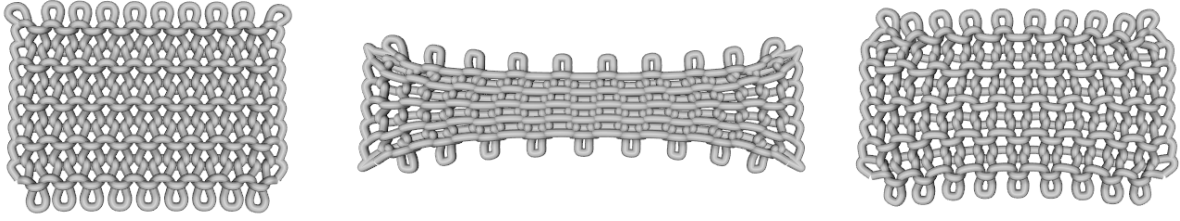


Figure 7: A small piece of fabric (left) is overly stretched to the point where inter-yarn friction cannot prevent yarn sliding (middle), and plastic deformations are evident when forces are released and the fabric goes back to rest (right).

Example	Loop width (mm)	Yarn radius R (mm)	Elastic mod. Y (Pa)	Bend. mod. B (Pa)	Wrap mod. k_w (Pa)	Sliding Fric. Coef. μ	Rayleigh damping (α, β)
Sweater (Fig. 1)	3	0.75	1e7	1e-3	1e-2	0.3	10, 0.01
Sleeveless Shirt (Fig. 8)	1	0.25	1e7	3e-4	1e-2	0.3	2, 0.1
Sleeveless Pullover (Fig. 5)	6	1.5	1e7	3e-4	1e-2	0.3	5, 0.01

Table 1: Parameter values used in our examples.

4.3 Sliding Friction and Stitch Length

The ability to model inter-yarn sliding with friction forces is one of the cornerstones of our method. For sliding friction, we follow the approach of Cirio et al. [2014], and model Coulomb friction on sliding coordinates using anchored springs. According to Coulomb’s model, friction force is limited by the amount of normal compression at inter-yarn contact, which Cirio et al. estimated by assuming static equilibrium of stretch and bending forces. For knitted cloth, we incorporate stitch wrapping forces in the estimation of inter-yarn normal compression. To estimate the normal force due to bending and stitch wrapping, we simply project the forces onto the estimated normal at each contact node. To estimate the normal force due to stretch, on the other hand, we offset nodes along the contact normal to account for yarn volume. Sliding friction is governed by the friction coefficient μ .

When the end node of one stitch contact slides, the other node should slide too to preserve the material length of the contact stitch and avoid artificial creation or deletion of material. We assume that the material length of stitch contacts remains constant, and we enforce this using a penalty energy. For a stitch contact between nodes \mathbf{q}_0 and \mathbf{q}_1 as shown in Fig. 6, with arc length $l = u_1 - u_0$ and rest length L , we define the energy as:

$$V = \frac{1}{2} k_l L \left(\frac{l}{L} - 1 \right)^2, \quad (3)$$

where k_l is the stiffness of the length constraint.

Yarn sliding is negligible under small forces, because friction keeps the yarns in place. However, sliding may indeed take place under moderate forces, such as extensive stretch. In that case, sliding produces plastic deformations that remain when forces are released. Fig. 7 shows an example where a small piece of fabric (left) is overly stretched to the point where yarns slide (middle), and plastic deformation is present when the fabric is released (right).

5 Results

We have integrated our model in the simulation algorithm proposed by Cirio et al. [2014]. With implicit integration, the regularity of the patterns produces a sparse system matrix with at most 11 non-zero 5x5 blocks per block-row. We handle blocks produced by collisions

and seams in a tail matrix. All our examples were executed on a 3.4 GHz Quad-core Intel Core i7-3770 CPU with 32GB of memory, with an NVIDIA Tesla K40 graphics card with 12GB of memory. Simulations were executed with a time step of 1ms, and the parameter values used in the large-scale examples are listed in Table 1. Please see our accompanying video for all animation results.

Sweater We dressed a dancing female mannequin (Fig. 1) with a sweater made of 56K loops (224353 stitch contact nodes). The sweater is knit in Garter style, with seams on the sides of the body, the shoulders, the sleeve-body junctions, and along the sleeves. In the textile industry, stitch density is measured as the number of stitches per inch, and is called Gauge (GG). Our sweater has 6.5 stitches per inch, a gauge commonly found in real sweaters. The simulation took 96 seconds per visual frame (at 30fps), roughly 7x faster than the approach by Kaldor et al. [2010] for a model of similar characteristics (without accounting for hardware differences).

Sleeveless T-shirt We used a sleeveless T-shirt model to dress a male mannequin performing highly dynamic karate motions (Fig. 8). The T-shirt has 325K loops (1.25M stitch contact nodes), 20 stitches per inch, and is knit in Garter style. This gauge (20 GG) is commonly found in off-the-shelf T-shirts made of carded cotton. The simulation took an average of 7.4 minutes per visual frame (at 30fps), showing how garments with life-like resolutions can be computed in tractable time with our approach.

Stockinette Curl The stockinette pattern produces a curl behavior in the fabric, and in our model this effect is captured by the stitch wrapping forces introduced in Section 4.2. We show the effect of curl in a stockinette garment in Fig. 5. The garment is a sleeveless wool pullover, with 8750 loops (34416 stitch contact nodes). As in real cloth, the curl effect is particularly visible at the edges of the fabric. Here, the lower edge and the collar wrap around themselves.

Rib Stretch Nonlinearities One of the main advantages of yarn-level models is the ability to naturally capture complex nonlinear deformations. Fig. 9 shows an example nonlinear behavior observed when stretching a piece of rib fabric, which appears compressed at rest, and with the characteristic ridges of the rib pattern. The plot shows the force applied to one side of the fabric vs. the side-to-side distance, and highlights the existence of 3 regimes dur-



Figure 8: Simulation of a high-resolution shirt with 325K loops (1.25M contact nodes, 6.25M DoFs), computed at 7.4 minutes per frame.

ing the deformation. First, the ridges are flattened, and stretch is opposed mainly by stitch wrapping forces. Second, the loops are deformed, and stretch is opposed mainly by yarn bending. And third, the yarns themselves are stretched. The nonlinear stretch behavior emerges naturally when using our yarn-level model thanks to the low-level structural representation and force models, but is difficult to capture using traditional mesh-based approaches.

6 Conclusions and Future Work

In this paper, we have presented an efficient method to simulate knitted cloth at the yarn level. We propose an efficient representation of knitted cloth that treats yarn-yarn contacts as persistent, thereby avoiding expensive contact handling altogether. Our compact discretization of stitch contacts allows us to capture the relevant yarn-level deformation modes, achieving complex, nonlinear and plastic effects at a macroscopic scale.

Although our model could handle any knit pattern based on purl and knit stitches between two yarns, there are many other patterns that exhibit more complex configurations [Yuksel et al. 2012]. These include yarn-overs, requiring a special treatment of friction forces, and increases and decreases, requiring loops with different numbers of stitch contacts. As for stitches involving multiple yarns, we believe that the persistent contact metaphor could also be extended to

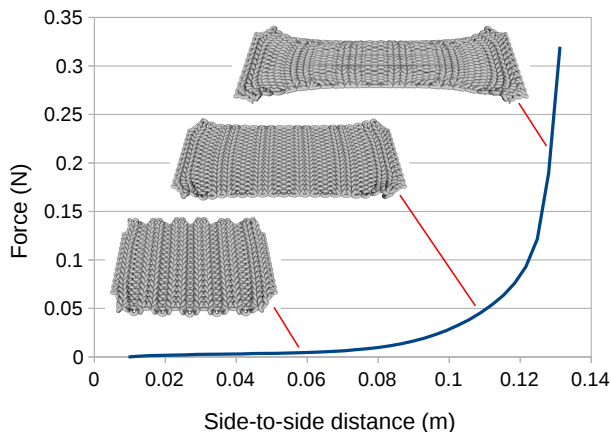


Figure 9: Force plot of a stretched rib fabric. The highly nonlinear behavior is evident, with three different regimes corresponding mainly to opposing wrapping, bending and stretching forces.

those cases, perhaps in a pair-wise manner.

In addition, our model omits twist, following observations from the textile literature, and our results seem to validate that it does not contribute to the main macroscopic effects. However, it would be interesting to analyze its actual effect, both in pre-twisted yarn assemblies, as well as during deformations that induce dynamic twist.

Finally, in our examples, model parameters are artist-tuned. In future work, we would like to estimate these parameters from example deformations, or derive them from more complex simulations with contact mechanics and physically based parameters.

Acknowledgements

We wish to thank Jaime González, Eder Miguel, Jesús Pérez and the GMRV group for diverse help with our submission, Wenzel Jacob for support with Mitsuba, and the Berkeley Garment Library [de Joya et al.] for the mannequin model and animations. This work was supported in part by the Spanish Ministry of Economy (TIN2012-35840) and the European Research Council (ERC-2011-StG-280135 Animetrics). The work of Gabriel Cirio and Jorge Lopez-Moreno was funded by the Spanish Ministry of Science and Education through Juan de la Cierva Fellowships.

References

- BREEN, D. E., HOUSE, D. H., AND WOZNY, M. J. 1994. Predicting the drape of woven cloth using interacting particles. In *Proceedings of the 21st Annual Conference on Computer Graphics and Interactive Techniques*, ACM, New York, NY, USA, SIGGRAPH '94, 365–372.
- CIRIO, G., LOPEZ-MORENO, J., MIRAUT, D., AND OTADUY, M. A. 2014. Yarn-level simulation of woven cloth. *ACM Trans. Graph.* 33, 6 (Nov.), 207:1–207:11.
- DE JOYA, J., NARAIN, R., O'BRIEN, J., SAMII, A., AND ZORDAN, V. Berkeley garment library. <http://graphics.berkeley.edu/resources/GarmentLibrary/>.
- DUAN, Y., KEEFE, M., BOGETTI, T. A., AND POWERS, B. 2006. Finite element modeling of transverse impact on a ballistic fabric. *International Journal of Mechanical Sciences* 48, 1, 33–43.
- DUHOVIC, M., AND BHATTACHARYYA, D. 2006. Simulating the deformation mechanisms of knitted fabric composites. *Composites Part A: Applied Science and Manufacturing* 37, 11.

ETZMUSS, O., KECKEISEN, M., AND STRASSER, W. 2003. A fast finite element solution for cloth modelling. In *Computer Graphics and Applications, 2003. Proceedings. 11th Pacific Conference on*, 244–251.

HEARLE, J. W. S., GROSBERG, P., AND BACKER, S. 1969. *Structural Mechanics of Fibers, Yarns, and Fabrics*, vol. 1. John Wiley & Sons Inc, New York.

JIANG, Y., AND CHEN, X. 2005. Geometric and algebraic algorithms for modelling yarn in woven fabrics. *Journal of the Textile Institute* 96, 4, 237–245.

KALDOR, J. M., JAMES, D. L., AND MARSCHNER, S. 2008. Simulating knitted cloth at the yarn level. *ACM Trans. Graph.* 27, 3, 65:165:9.

KALDOR, J. M., JAMES, D. L., AND MARSCHNER, S. 2010. Efficient yarn-based cloth with adaptive contact linearization. *ACM Transactions on Graphics* 29, 4 (July), 105:1–105:10.

KAWABATA, S., NIWA, M., AND KAWAI, H. 1973. The finite-deformation theory of plain-weave fabrics part i: The biaxial-deformation theory. *Journal of the Textile Institute* 64, 1, 21–46.

KING, M. J., JEARANAISILAWONG, P., AND SOCRATE, S. 2005. A continuum constitutive model for the mechanical behavior of woven fabrics. *International Journal of Solids and Structures* 42, 13, 3867–3896.

MCGLOCKTON, M. A., COX, B. N., AND MCMEEKING, R. M. 2003. A binary model of textile composites: III high failure strain and work of fracture in 3D weaves. *Journal of the Mechanics and Physics of Solids* 51, 8, 1573–1600.

NADLER, B., PAPADOPOULOS, P., AND STEIGMANN, D. J. 2006. Multiscale constitutive modeling and numerical simulation of fabric material. *International Journal of Solids and Structures* 43, 2, 206 – 221.

NG, S.-P., TSE, P.-C., AND LAU, K.-J. 1998. Numerical and experimental determination of in-plane elastic properties of 2/2 twill weave fabric composites. *Composites Part B: Engineering* 29, 6, 735–744.

NOCENT, O., NOURRIT, J.-M., AND REMION, Y. 2001. Towards mechanical level of detail for knitwear simulation. In *Winter School in Computer Graphics and Visualization*, 252–259.

PAGE, J., AND WANG, J. 2000. Prediction of shear force and an analysis of yarn slippage for a plain-weave carbon fabric in a bias extension state. *Composites Science and Technology* 60, 7, 977 – 986.

PAN, N., AND BROOKSTEIN, D. 2002. Physical properties of twisted structures. ii. industrial yarns, cords, and ropes. *Journal of Applied Polymer Science* 83, 3, 610–630.

PARSONS, E. M., KING, M. J., AND SOCRATE, S. 2013. Modeling yarn slip in woven fabric at the continuum level: Simulations of ballistic impact. *Journal of the Mechanics and Physics of Solids* 61, 1, 265–292.

PEIRCE, F. T. 1937. The geometry of cloth structure. *Journal of the Textile Institute Transactions* 28, 3, T45–T96.

PROVOT, X. 1995. Deformation constraints in a mass-spring model to describe rigid cloth behavior. In *In Graphics Interface*, 147–154.

REESE, S. 2003. Anisotropic elastoplastic material behavior in fabric structures. In *IUTAM Symposium on Computational Mechanics of Solid Materials at Large Strains*, C. Miehe, Ed., no. 108

in *Solid Mechanics and Its Applications*. Springer Netherlands, 201–210.

REMION, Y., NOURRIT, J.-M., AND GILLARD, D. 1999. Dynamic animation of spline like objects. In *Winter School in Computer Graphics and Visualization*, 426–432.

RENKENS, W., AND KYOSEV, Y. 2011. Geometry modelling of warp knitted fabrics with 3d form. *Textile Research Journal* 81, 4, 437–443.

SUEDA, S., JONES, G. L., LEVIN, D. I. W., AND PAI, D. K. 2011. Large-scale dynamic simulation of highly constrained strands. *ACM Trans. Graph.* 30, 4, 39:1–39:10.

XIA, W., AND NADLER, B. 2011. Three-scale modeling and numerical simulations of fabric materials. *International Journal of Engineering Science* 49, 3, 229–239.

YUKSEL, C., KALDOR, J. M., JAMES, D. L., AND MARSCHNER, S. 2012. Stitch meshes for modeling knitted clothing with yarn-level detail. *ACM Trans. Graph.* 31, 4, 37:1–37:12.

A Stitch Wrapping Forces and Jacobians

The central axis of the stitch is defined by a vector

$$\mathbf{e} = \frac{\mathbf{x}_1 - \mathbf{x}_0}{\|\mathbf{x}_1 - \mathbf{x}_0\|}, \quad (4)$$

with derivatives

$$\frac{\partial \mathbf{e}}{\partial \mathbf{x}_0} = -\frac{1}{\|\mathbf{x}_1 - \mathbf{x}_0\|} (\mathbf{I} - \mathbf{e} \mathbf{e}^T) \quad \text{and} \quad \frac{\partial \mathbf{e}}{\partial \mathbf{x}_1} = -\frac{\partial \mathbf{e}}{\partial \mathbf{x}_0}. \quad (5)$$

The triangles $(\mathbf{q}_0, \mathbf{q}_1, \mathbf{q}_4)$ and $(\mathbf{q}_0, \mathbf{q}_3, \mathbf{q}_1)$ have normal vectors

$$\mathbf{n}_a = \frac{\mathbf{v}_a}{\|\mathbf{v}_a\|}, \quad \text{with } \mathbf{v}_a = (\mathbf{x}_4 - \mathbf{x}_1) \times (\mathbf{x}_0 - \mathbf{x}_1). \quad (6)$$

$$\mathbf{n}_b = \frac{\mathbf{v}_b}{\|\mathbf{v}_b\|}, \quad \text{with } \mathbf{v}_b = (\mathbf{x}_0 - \mathbf{x}_1) \times (\mathbf{x}_3 - \mathbf{x}_1). \quad (7)$$

It is convenient to define the auxiliary vectors

$$\mathbf{x}_{a0} = \mathbf{x}_4 - \mathbf{x}_1, \quad \mathbf{x}_{a1} = \mathbf{x}_0 - \mathbf{x}_4, \quad \text{and} \quad \mathbf{x}_{a4} = \mathbf{x}_1 - \mathbf{x}_0. \quad (8)$$

$$\mathbf{x}_{b0} = \mathbf{x}_1 - \mathbf{x}_3, \quad \mathbf{x}_{b1} = \mathbf{x}_3 - \mathbf{x}_0, \quad \text{and} \quad \mathbf{x}_{b3} = \mathbf{x}_0 - \mathbf{x}_1. \quad (9)$$

Their derivatives, $\frac{\partial \mathbf{x}_{ai}}{\partial \mathbf{x}_j}$ and $\frac{\partial \mathbf{x}_{bi}}{\partial \mathbf{x}_j}$, can take the values $\{\mathbf{I}, -\mathbf{I}, \mathbf{0}\}$.

The wrapping angle between the triangles is

$$\psi = \arccos(\mathbf{n}_a^T \mathbf{n}_b), \quad (10)$$

and its derivatives take the form

$$\frac{\partial \psi}{\partial \mathbf{x}_i} = \frac{1}{\|\mathbf{v}_b\|} \mathbf{n}_b^T \mathbf{e}^T \mathbf{x}_{bi} - \frac{1}{\|\mathbf{v}_a\|} \mathbf{n}_a^T \mathbf{e}^T \mathbf{x}_{ai}. \quad (11)$$

From the potential energy in (2), forces on contact nodes ($i \in \{0, 1, 3, 4\}$) are computed as:

$$\mathbf{F}_{\mathbf{x}_i} = -k_w L (\psi - \psi_0) \left(\frac{\mathbf{x}_{bi}^T}{\|\mathbf{v}_b\|} \mathbf{e} \mathbf{n}_b - \frac{\mathbf{x}_{ai}^T}{\|\mathbf{v}_a\|} \mathbf{e} \mathbf{n}_a \right). \quad (12)$$

And their Jacobians take the form:

$$\begin{aligned} \frac{\partial \mathbf{F}_{\mathbf{x}_i}}{\partial \mathbf{x}_j} = & -k_w L \left(\frac{\mathbf{x}_{bi}^T}{\|\mathbf{v}_b\|} \mathbf{e} \mathbf{n}_b - \frac{\mathbf{x}_{ai}^T}{\|\mathbf{v}_a\|} \mathbf{e} \mathbf{n}_a \right) \left(\frac{\mathbf{x}_{bj}^T}{\|\mathbf{v}_b\|} \mathbf{e} \mathbf{n}_b - \frac{\mathbf{x}_{aj}^T}{\|\mathbf{v}_a\|} \mathbf{e} \mathbf{n}_a \right)^T \\ & - \frac{k_w L (\psi - \psi_0)}{\|\mathbf{v}_b\|} \left(\frac{\mathbf{x}_{bi}^T}{\|\mathbf{v}_b\|} \mathbf{e} (\mathbf{I} - 2 \mathbf{n}_b \mathbf{n}_b^T) \mathbf{x}_{bj}^* + \mathbf{n}_b \mathbf{x}_{bi}^T \frac{\partial \mathbf{e}}{\partial \mathbf{x}_j} + \mathbf{n}_b \mathbf{e}^T \frac{\partial \mathbf{x}_{bi}}{\partial \mathbf{x}_j} \right) \\ & + \frac{k_w L (\psi - \psi_0)}{\|\mathbf{v}_a\|} \left(\frac{\mathbf{x}_{ai}^T}{\|\mathbf{v}_a\|} \mathbf{e} (\mathbf{I} - 2 \mathbf{n}_a \mathbf{n}_a^T) \mathbf{x}_{aj}^* + \mathbf{n}_a \mathbf{x}_{ai}^T \frac{\partial \mathbf{e}}{\partial \mathbf{x}_j} + \mathbf{n}_a \mathbf{e}^T \frac{\partial \mathbf{x}_{ai}}{\partial \mathbf{x}_j} \right), \end{aligned} \quad (13)$$

where \mathbf{u}^* denotes the cross product matrix for vector \mathbf{u} .